European Heart Journal Advance Access published January 12, 2016

European Heart Journal
doi:10.1093/eurheartj/ehv711

CLINICAL RESEARCH
Acute coronary syndromes

Mechanisms of stent thrombosis analysed by optical coherence tomography: insights from the national PESTO French registry

Geraud Souteyrand[1,2†*], Nicolas Amabile[3†], Lionel Mangin[4], Xavier Chabin[1,2], Nicolas Meneveau[5], Guillaume Cayla[6], Gerald Vanzetto[7], Pierre Barnay[8], Charlotte Trouillet[9], Gilles Rioufol[10], Gregoire Rangé[11], Emmanuel Teiger[12], Regis Delaunay[13], Olivier Dubreuil[14], Thibault Lhermusier[15], Aurélien Mulliez[16], Sebastien Levesque[17], Loic Belle[4], Christophe Caussin[3] and Pascal Motreff[1,2], on the Behalf of the PESTO Investigators

[1]Cardiology Department, CHU Clermont-Ferrand, Clermont-Ferrand 63000, France; [2]Cardio Vascular Interventional Therapy and Imaging (CaVITI), UMR CNRS 6284, Auvergne University, Clermont-Ferrand, France; [3]Cardiology Department, Institut Mutualiste Montsouris, Paris, France; [4]Cardiology Department, CH Annecy, Annecy, France; [5]Cardiology Department, CHU Besançon, Besançon, France; [6]Cardiology Department, CHU Nimes, Nimes, France; [7]Cardiology Department, CHU Grenoble, Grenoble, France; [8]Cardiology Department, CH Henri Duffaut, Avignon, France; [9]Cardiology Department, CH La Rochelle-Re-Aunis, La Rochelle, France; [10]Cardiology Department, Hospices Civils de Lyon, Bron, France; [11]Cardiology Department, CH Chartres, Chartres, France; [12]Cardiology Department, CHU Henri Mondor-Assistance Publique-Hôpitaux de Paris, Creteil, France; [13]Cardiology Department, CH St Brieuc, St Brieuc, France; [14]Cardiology Department, St Luc-St Joseph hospital, Lyon, France; [15]Department of Cardiology, CHU Rangueil, Toulouse, France; [16]Bio-Statistics Unit, délégation recherche clinique & innovation, CHU de Clermont-Ferrand, France; and [17]Cardiology Department, CHU Poitiers, Poitiers, France

Received 19 April 2015; revised 25 November 2015; accepted 3 December 2015

Aims Angiography has limited value for identifying the causes of stent thrombosis (ST). We studied a large cohort of patients by optical coherence tomography (OCT) to explore ST characteristics and mechanisms.

Methods and results A prospective multicentre registry was screened for patients with confirmed ST. Optical coherence tomography was performed after initial intervention to the culprit lesion (in 69% of cases in a deferred procedure). Stent thrombosis was classified as acute (AST), sub-acute (SAST), late (LST), and very late (VLST). Optical coherence tomography records were analysed in a central core lab. The analysis included 120 subjects aged 61.7 [51.4–70.7]; 89% male. Very late ST was the clinical presentation in 75%, LST in 6%, SAST in 15%, and AST in 4% of patients. Bare metal stents (BMS) were used in 39%, drug-eluting stents (DES) in 59% and bioresorbable vascular scaffolds in 2% of the cases. Optical coherence tomography identified an underlying morphological abnormality in 97% of cases, including struts malapposition (34%), neoatherosclerotic lesions (22%), major stent underexpansion (11%), coronary evagination (8%), isolated uncovered struts (8%), edge-related disease progression (8%), and neointimal hyperplasia (4%). Ruptured neoatherosclerotic lesions were more frequent with BMS than with DES (36 vs. 14%, $P = 0.005$), whereas coronary evaginations were more frequent with DES than with BMS (12 vs. 2%, $P = 0.04$). LST + VLST were mainly related to malapposition (31%) and neoatherosclerosis (28%), while prominent mechanisms for AST + SAST were malapposition (48%) and underexpansion (26%).

Conclusion In patients with confirmed ST, OCT imaging identified an underlying morphological abnormality in 97% of cases.

Keywords Optical coherence tomography • Stent thrombosis • Drug-eluting stent • Bare metal stent

Clinical summary

Angiography is of limited use in identifying the underlying mechanisms of stent thrombosis. Optical coherence tomography could help to find mechanical abnormalities and may help guide management of patients.

* Corresponding author. Tel: +33 473751308, Fax: +33 473751417, Email: gsouteyrand@chu-clermontferrand.fr

† Both authors contributed equally to the paper.

Introduction

Despite improvements in device design and anti-platelet therapy (APT) over the past decades, stent thrombosis (ST) remains a persistent complication of percutaneous coronary interventions (PCIs). Although recent data indicate that the overall incidence rate may be no more than 1% per year (and even lower in case of very late ST),[1] the potential consequences can be devastating, including high mortality.[2,3]

The pathophysiology of ST is not fully understood.[3] A number of factors may trigger ST including stent design, comorbidities such as diabetes, patients' compliance with APT, high on treatment platelet reactivity, and lesion morphology.[2]

The mechanisms promoting ST vary with increasing time from PCI. In recent years, the use of intra-vascular imaging has revealed additional causes of ST: whereas underexpansion and malapposition appear to be leading causes of acute ST (AST), and sub-acute ST (SAST),[4] neoatherosclerosis has been shown to be a major contributor to very late ST (VLST).[5,6] The exact role of uncovered struts in ST has not been completely elucidated but uncovered stent struts have been shown to be independently associated with late drug-eluting stent (DES) thrombosis.[7] Moreover, malapposition seems to be more frequent after DES implantation than after Bare metal stents (BMS) due to expansive vascular remodelling[8] and might also trigger ST.[9]

Coronary angiography is often of limited value in the identification of different mechanisms underlying ST and as a guide to adequate therapy. Recently, optical coherence tomography (OCT) has been noted as a potentially important imaging technique to assess mechanism of stent failure.[10] Optical coherence tomography offers high resolution (10–15 μm) as well as *in vivo* coronary plaque morphology visualization. However, this method has not been used in large-scale multicentre prospective studies.

The PESTO (Morphological Parameters Explaining Stent Thrombosis assessed by OCT) registry was set up to investigate the usefulness of OCT in assessing characteristics, mechanisms, and relative incidence of ST among a large cohort of patients.

Methods

Patients

The PESTO multicentre prospective observational registry included patients from 29 French catheterization facilities from January 2013 to October 2014. Patients who were referred with acute coronary syndromes (ACS) were prospectively screened for the presence of confirmed ST. The definite diagnosis of ST was made after the angiogram in accordance with the Academic Research Consortium ST definitions[10] and classified as AST, SAST, LST, and VLST, using standard definitions.[11]

Patients' baseline characteristics including medical history, clinical, biological, and angiographic parameters and recent modification of APT were prospectively collected in a predefined standardized case report form. As a part of the protocol, the PESTO local investigators reported and classified the ST suspected mechanism into three categories ('unidentified', 'probably identified', and 'completely identified') before (i.e. based on angiography data alone) and after OCT imaging.

The study complied with the Declaration of Helsinki. The Gabriel Montpied University Hospital's Ethics Committee approved the research protocol and informed consent was obtained from each patient before inclusion.

Acute coronary syndrome management

All patients included in the study were routinely treated with oral anti-platelet therapy including aspirin and clopidogrel, or prasugrel or ticagrelor. Parenteral anti-thrombotic therapy includes abciximab, unfractionated, or low-weight heparin in accordance with the European Society of Cardiology (ESC) guidelines for management of patients with STEMI and NSTEMI.[12]

Percutaneous coronary intervention was performed with a 6 Fr guiding catheter in all patients. The decision whether to use a thromboaspiration device and the options for ST management (culprit lesion deocclusion, balloon dilation alone, redo stenting, or medical treatment with anticoagulant therapy) were at the discretion of the local operators. The timing for OCT imaging (*ad hoc* or deferred analysis) was not pre-specified by the study protocol and was chosen by the local investigators according to their experience and patients' clinical and angiography characteristics.

Percutaneous coronary intervention and frequency domain-optical coherence tomography images acquisition

Frequency domain-OCT (FD-OCT) images were acquired using a commercially available system (C7 System; LightLab Imaging Inc/St Jude Medical, Westford, MA) in all facilities as previously described.[6] Frequency domain-OCT imaging was performed immediately following restoration of thrombolysis in myocardial infarction (TIMI) 3 flow or during deferred control angiography.[13]

Frequency domain-optical coherence tomography image analysis

Offline analysis was performed with proprietary software (Lightlab, Imaging Inc/St Jude Medical) after confirming calibration settings of the Z-offset. All images were recorded digitally, stored and read by three independent investigators (G.S., N.A., P.M./blinded to patients' clinical, ST type and angiographic baseline characteristics) in a centralized core laboratory. Discordances around the leading cause of ST were resolved by consensus. The aetiologies of mechanical ST were classified as: major stent malapposition, severe stent underexpansion, in-stent ruptured neoatherosclerosis, coronary evaginations, isolated uncovered struts without associated abnormality, edge dissection, edge-related disease progression, and intra-stent neointimal hyperplasia with adherent thrombus (*Figure 1*).

The region of interest, including the stented as well as the surrounding normal coronary artery segments, was analysed systematically at 1 mm intervals. The outlines of stent and lumen were drawn for area measurements. In the presence of thrombus with low attenuation, the visible lumen contour could still be drawn behind the thrombus. In the presence of thrombus with high attenuation, the lumen contour was allowed to be extrapolated behind the thrombus when the lumen contour was visible in >3 quadrants. The stent area (SA) was measured by joining the middle points of the endoluminal signal rich strut surface of the stent. In case the stent was covered by thrombus with high signal attenuation, the SA was delineated only if at least one strut was clearly visible in every quadrant. Stent area and intra-stent lumen area (intra-stent area/ISA) were measured for each interval within the stent. Proximal and distal references lumen areas were also determined. The most 'normal-appearing' segments 5 mm proximal and distal to the lesion shoulders identified by OCT were used as references.

Thrombi were defined as masses attached of the vessel wall or stent and protruding into the vessel lumen, and were characterized according to previous reports.[14] White thrombus was identified as signal rich, low-backscattering mass. Red thrombus was identified as high-backscattering

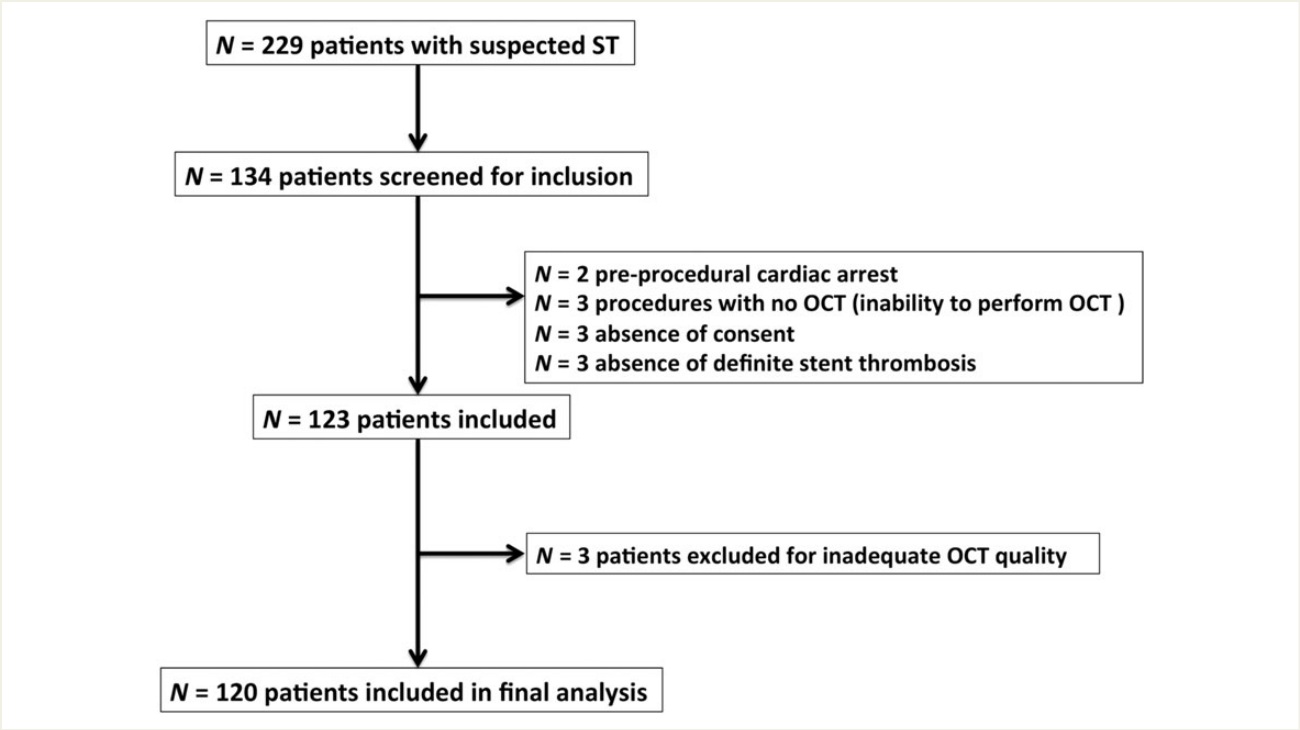

Figure 1 Workflow of the study.

protrusions inside the lumen of the artery, with signal-free shadowing in the OCT. The thrombus score was graded, according to the method proposed by the ESC OCT expert review document,[15] based on semi-quantitative assessment of thrombus (number of involved quadrants in the cross-sectional OCT images) and the longitudinal extension of the thrombus itself. By applying this method in each cross-section, a thrombus was classified as absent or subtending 1, 2, 3, or 4 quadrants. The global OCT-thrombus score was then calculated as the sum of each cross-sectional score.[15,16]

Neointimal thickness (per strut) and area (per cross-sectional area) were calculated as previously reported.[6] An uncovered strut was defined as a strut of measured neointimal thickness equal to 0 μm.[15] In the presence of a highly attenuating layer of thrombus, struts were categorized as not analysable for coverage. A malapposed strut was defined as a strut with a measured distance between its surface and the adjacent vessel surface greater than the strut thickness for BMS or greater than the sum of the thickness of the strut plus polymer for DES.[15] The malapposition was considered significant if the stent lumen distance was $\geq$200 μm.[4]

A coronary evagination was defined as the presence of an outward bulge in the luminal vessel contour between apposed struts with a maximum depth of the bulge exceeding that of the actual strut thickness.[17] Intimal vessels (or micro-channels) were defined as sharply delineated poor signal voids that could be followed in multiple contiguous frames. Neo-atheroma was defined as the combination of neointimal diffuse thickening with atherosclerotic plaque architectural features including lipid-laden intima, presence of a fibrous cap, neovessels and potential neointimal rupture.[6] Neointimal rupture referred to a break in the fibrous cap connecting the lumen with the underlying lipid pool.[18] Severe stent underexpansion was defined as intra-stent minimal area $\leq$70% of the average reference lumen area or $\leq$80% of the lumen area of the reference segment with the lowest lumen area.[19] Edge-related disease progression was defined as the presence of a ruptured necrotic core plaque at the proximal edge of the stent in an incompletely covered lesion.

Endpoints definition

The primary endpoint was the presence of an underlying mechanical abnormality (malapposition, severe underexpansion, ruptured neoatherosclerotic lesion, coronary evagination, edge-related disease progression, neointimal hyperplasia with adherent thrombus, persistent edge dissection, or isolated uncovered struts without presence of any of the preceding abnormalities) on OCT analysis in patients with definite ST. The secondary endpoint was the incidence of major adverse cardiovascular events (including cardiovascular death, non-fatal stroke, non-fatal myocardial infarction, and the need for urgent target vessel revascularization) during 180 days after hospital discharge following ST. Follow-up was by clinic visits and/or by telephone contact.

Statistical analysis

The statistical analysis was performed with SPSS 21.0 software (SPSS software, Chicago, IL, USA). Continuous variables are expressed as median and interquartile ranges and the normality of their distributions was assessed by the Kolmogorov–Smirnov test. The inter-observer (analyst #1 vs. analyst #2; analyst #1 vs. analyst #3; analyst #2 vs. analyst #3) and intra-observer reproducibility was evaluated by the kappa coefficient with calculation of the 95% confidence interval and tested vs. the null hypothesis. The differences between ST mechanical underlying abnormalities and OCT quantitative parameters were compared using χ^2 or Fisher exact tests (for categorical variables) and Student's *t* or *U* Mann–Whitney tests (for continuous variables), as appropriate. Incidence of the secondary endpoint and of cardiovascular death during follow-up was evaluated according to the Kaplan–Meier method. A two-sided α level of 0.05 was used for all superiority testing.

Table 1 Baseline characteristics of the population

	All patients (*N* = 120)	BMS (*n* = 47)	DES (*n* = 71)	*P**
Age (years)	61.7 ± 19.3	61.0 ± 16.0	62.0 ± 20.7	0.61
Male gender (%)	89	87	90	0.62
Cardiovascular risk factors				
Active smoking (%)	35	42	29	0.12
Dyslipidaemia (%)	86	78	82	0.65
Hypertension (%)	56	35	72	<0.001
Diabetes (%)	34	15	38	0.10
Overweight status (%)	62	58	67	0.29
Presentation mode				
STEMI (%)	82	78	85	0.39
NSTEMI (%)	17	20	15	0.57
Index PCI to ST delay (years)	2.6 ± 6.1	6.5 ± 9.5	2.5 ± 3.5	*0.006*
Acute ST (%)	4	6	3	0.31
Sub-acute ST (%)	15	13	15	0.68
Late ST (%)	6	9	3	0.17
Very late ST (%)	75	72	79	0.41
Culprit stent characteristics				
LAD localization (%)	56	32	55	0.01
Circumflex localization (%)	23	21	18	0.69
RCA localization (%)	41	47	27	0.03
Length (mm)	20.0 ± 8.0	18.0 ± 7.8	23.0 ± 6.0	0.04
Diameter (mm)	3.0 ± 0.5	3.0 ± 1	3.0 ± 0.75	*0.005*
Bifurcation lesion (%)	19	17	21	0.56
Initial implantation for ACS (%)	73	86	63	0.008
Current medication at the time of ST				
Statins (%)	85	77	89	0.08
β-Blockers (%)	71	65	74	0.31
Calcium channels blockers (%)	21	16	24	0.32
ACE inhibitors (%)	41	47	36	0.29
ARA (%)	19	7	27	0.009
Aspirin (%)	76	66	82	0.05
Clopidogrel (%)	28	26	31	0.52
Ticagrelor (%)	5	4	3	0.65
Prasugrel (%)	2.5	2	3	0.52
Double APT (%)	24	21	24	0.74
Single APT (%)	63	57	67	0.26
No APT (%)	13	21	9	0.05
Oral anticoagulant therapy (%)	8	7	9	0.52

ACE, angiotensin converting enzyme; ACS, acute coronary syndromes; ARA, angiotensin II receptor antagonists; APT, antiplatelet therapy; BMS, bare metal stents; BVS, bioresorbable vascular scaffold; DES, drug-eluting stents; LAD, left anterior descending artery; NSTEMI, non-ST elevation myocardial infarction; RCA, right coronary artery; ST, stent thrombosis; STEMI, ST elevation myocardial infarction.
*P-value is for comparison BMS vs. DES by *U* Mann–Whitney test.

Results

Baseline characteristics

A total of 229 patients in 17 active centres were treated for ST during the inclusion period. A hundred and thirty-four patients were screened and of these, 123 provided informed consent (*Figure 1*). Three patients (2.4%) were excluded from the analysis because of inadequate OCT image quality (*Figure 1*). The baseline characteristics of the 120 patients included in the final analysis are given in *Table 1*.

Most patients presented with VLST. The average time between index PCI and ST was 4.4 ± 0.4 years. Most devices were DES in 59% and BMS in 39%. Bioresorbable vascular scaffold (BVS)

thrombosis was determined in two patients. First-generation DES were implicated in 34 subjects, second-generation DES in 35 subjects, and third-generation DES in two subjects. Patients with DES-related ST had a significantly higher incidence of hypertension, shorter time from index PCI to ST, longer and smaller devices and a more frequent left anterior descending artery location than patients with BMS. Single or dual APT was used by 87% of patients at the time of thrombosis (*Table 1*). A recent (<15 days) modification of APT was reported in 22% of patients prior to ST.

The initial antegrade TIMI flow was Grade 0 in 71%, Grade 1 in 10%, Grade 2 in 5%, and Grade 3 in 14% of patients. The method of initial intervention to the culprit lesion was manual thrombectomy in 101 patients (median number of passes: 2 [1–3]). Intravenous glycoprotein IIb–IIIa inhibitor therapy was administered to 89 subjects. Optical coherence tomography images were acquired during a deferred procedure in 85 patients (69%) (median delay between deocclusion to OCT: 4.0 days [2–7]).

Optical coherence tomography analysis of mechanisms underlying stent thrombosis

A total of 26 166 struts were analysed. Due to highly attenuating thrombus, 1235 struts in 120 patients could not be analysed. The intra- and inter-observer reproducibility for assessing the leading cause of ST was high for all reviewers (kappa coefficient ≥ 0.8, $P < 0.001$). The primary endpoint (underlying morphological abnormality) was identified in 96.7% of patients. The remaining four cases (no mechanical cause identified) were related to APT interruption during the first month following stent implantation. A unique abnormality was found in 77.5% and multiple abnormalities in 22.5% of the cases. Physicians' interpretations of OCT data correlated with those of the core lab in 84 of 120 cases (70%): these discrepancies suggest individual differences in OCT interpretation experience.

Struts malapposition was the most frequently observed abnormality and was highly prevalent throughout all ST types (*Table 2*). Ruptured neoatherosclerosis was significantly more frequently observed in LST + VLST patients, whereas severe underexpansion was more common in subjects with AST + SAST (*Figure 2*).

The causes and underlying mechanisms of ST varied according to stent type (*Tables 3* and *4*). Coronary evaginations were more frequently observed in DES than in BMS, whereas the incidence of ruptured neoatherosclerosis lesions was higher in BMS than in DES. The delay between index PCI and ST was longer in the BMS neoatherosclerosis group than in the DES one (10.6 [8.8–14.8] vs. 5.3 [2.4–7.0] years, $P = 0.001$). However, malapposition remained the main observed abnormality, regardless of the type of stent. The two cases of acute/sub-acute BVS thrombosis were related to severe underexpansion.

Stent thrombosis management and clinical follow-up

Before OCT, the mechanism of ST was considered as 'completely identified' in 12% of patients by local operators; this increased to 41% after OCT. Mechanisms were 'probably identified' in 40% before and 46% after OCT. The percentage of patients with 'unidentified' mechanisms was reduced from 48% without OCT to 13% with OCT. These differences were statistically significant ($P < 0.001$).

Balloon angioplasty alone in 37%, repeat stenting in 31% and further additional thromboaspiration in 2% of the cases. The left ventricular ejection fraction at discharge was 55% [45–60].

Follow-up data were obtained in 122 (99%) patients. The rates of survival and freedom from MACE at 6 months were 97.4% [95% CI: 95.9–98.9%] and 91.5% [95% CI: 88.9–94.1%], respectively. During this period, a total of 12 adverse events were recorded (none during the in-hospital phase): three subjects died, eight underwent urgent target vessel revascularization (including three recurrent ST), and one subject experienced a transient ischaemic attack.

Discussion

The PESTO multicentre national registry was designed to evaluate the value of OCT techniques to improve the understanding of the clinical presentation and mechanisms underlying ST.[20] The present work represents the largest attempt to date to explore the aetiology of this rare clinical event by OCT techniques.

Table 2 Stent thrombosis underlying mechanisms according to clinical presentation

	All patients ($n = 120$)	AST ($n = 5$)	SAST ($n = 18$)	LST ($n = 7$)	VLST ($n = 90$)	A + SAST ($n = 23$)	L + VLST ($n = 97$)	P*
Malapposition (%)	34	60	44	44	30	48	32	0.12
Ruptured NA (%)	23	0	0	14	29	0	28	0.004
Severe underexpansion (%)	11	20	28	14	7	26	7	0.02
Coronary evaginations (%)	8	0	0	14	10	0	10	0.11
ER disease progression (%)	8	0	6	0	9	4	8	0.45
Isolated uncovered struts (%)	8	0	0	0	11	0	10	0.11
NIH with thrombus (%)	4	0	0	14	4	0	5	0.34
Edge dissection (%)	1	20	0	0	0	4	0	0.19
No cause identified (%)	3	0	22	0	0	18	0	0.001

AST, acute stent thrombosis; ER, edge related; LST, late stent thrombosis; NA, neoatherosclerosis; NIH, neointimal hyperplasia; SAST, sub-acute stent thrombosis; VLST, very late stent thrombosis.
*P-value is for comparison A + SAST vs. L + VLST.

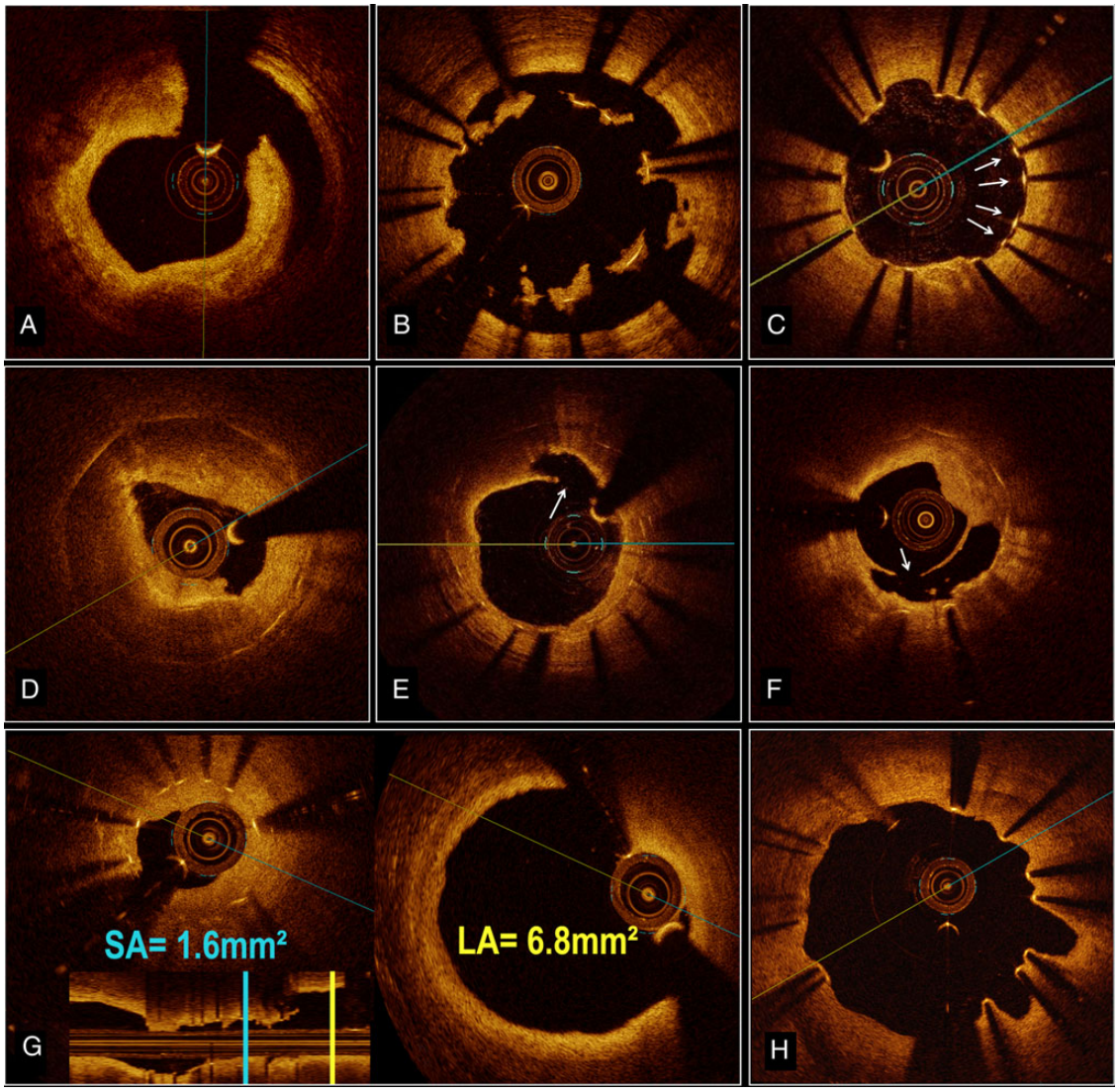

Figure 2 Representative examples of stent thrombosis underlying mechanisms explored by optical coherence tomography imaging after optimal thrombus resorption: acute stent thrombosis: edge dissection (*A*); sub-acute stent thrombosis: stent major malapposition (*B*); late stent thrombosis: isolated uncovered struts (*C*); very late stent thrombosis: neoatherosclerosis lesion (*D*); ruptured neoatherosclerotic lesion (*E* and *F*); major stent underexpansion with stent area and reference lumen area measurements (*G*); coronary evaginations related to underlying positive remodelling (*H*).

Table 3 Stent thrombosis underlying mechanisms according to stent type

	All patients (n = 120)	BMS (n = 47)	DES (n = 71)	P
Malapposition (%)	34	32	36	0.71
Ruptured NA (%)	23	36	14	0.005
Severe underexpansion (%)	11	6	13	0.22
Coronary evaginations (%)	8	3	13	0.04
ER disease progression (%)	8	13	4	0.09
Isolated uncovered struts (%)	8	4	11	0.16
NIH with thrombus (%)	4	4	4	0.67
Edge dissection (%)	1	0	1	0.61
No cause identified (%)	3	2	4	0.48

Table 4 Quantitative optical coherence tomography data (data are expressed as median ± interquartile range)

	Stent length	Thrombotic score	No. of struts analysed per lesion	Min. lum. area (mm^2)	Mean lum. area (mm^2)	Min. IS area (mm^2)	Mean IS area (mm^2)	Mean NI thickness (μm)	Malapposed struts (%)	Maximal malapposition (μm)	Uncovered struts (%)
Per underlying mechanism											
Malapposition ($n = 39$)	20.0 ± 8.5	22.0 ± 14.0	186 ± 111	4.9 ± 2.2	6.53 ± 3.0	5.7 ± 3.1	6.5 ± 2.5	178 ± 160	12.7 ± 12.9	710 ± 670	21.2 ± 35.8
Ruptured NA ($n = 27$)	19.0 ± 9.5	9.0 ± 13.0	148 ± 98	2.0 ± 1.8	4.9 ± 2.7	6.2 ± 1.8	7.9 ± 1.7	412 ± 348	0 ± 3.8	0 ± 320	1.3 ± 11.3
Severe underexpansion ($n = 13$)	22.0 ± 11.0	13.0 ± 22.0	229 ± 150	2.1 ± 3.1	3.3 ± 2.6	2.9 ± 2.8	4.2 ± 2.6	137 ± 138	2.5 ± 9.2	365 ± 940	39.1 ± 53.7
Coronary evaginations ($n = 10$)	23.5 ± 11.0	14.5 ± 21.0	285 ± 83	4.3 ± 2.3	6.2 ± 1.7	4.6 ± 2.0	6.4 ± 3.5	94 ± 78	7.8 ± 12.6	340 ± 569	49.5 ± 25.4
ER disease progression ($n = 10$)	18.0 ± 10.0	6.0 ± 47.0	178 ± 109	4.0 ± 3.3	5.0 ± 3.6	5.1 ± 3.2	7.7 ± 3.4	250 ± 250	0 ± 4.5	0 ± 260	13.6 ± 34.6
Isolated uncovered struts ($n = 10$)	18.0 ± 8.5	5.5 ± 14.0	190 ± 91	4.2 ± 2.2	5.8 ± 2.6	5.9 ± 4.0	6.6 ± 4.5	123 ± 101	0 ± 2.2	0 ± 252	34.5 ± 30.7
NIH with thrombus ($n = 6$)	22.5 ± 15.5	10.0 ± 13.5	185 ± 404	2.0 ± 1.5	3.3 ± 0.8	4.9 ± 2.7	6.2 ± 3.1	349 ± 418	0	0	6.2 ± 17.1
Edge dissection ($n = 1$)	24	38	162	3.4	5.0	3.5	4.9	103	14.8	220	50.6
No cause identified ($n = 4$)	20.0 ± 9.5	16 ± 41	225 ± 123	4.3 ± 6.4	5.1 ± 7.1	5.5 ± 5	7.0 ± 4.6	25 ± 64	0.8 ± 1.9	85 ± 193	74.9 ± 59.6
Per clinical presentation											
A + SAST ($n = 23$)	22.0 ± 7.5	25.0 ± 29.5	180 ± 142	4.6 ± 2.4	5.4 ± 2.3	4.2 ± 2.6	5.6 ± 3.4	40 ± 101	6.7 ± 12.2	485 ± 517	43.4 ± 61.1
LST + VLST ($n = 97$)	20.0 ± 8	11.0 ± 19*	194 ± 117	3.3 ± 2.9	5.6 ± 3.0	5.8 ± 2.7**	7.1 ± 2.8**	231 ± 194*	2.9 ± 12.1	240 ± 677	15.3 ± 33.5*
Per stent type											
Overall											
BMS ($n = 47$)	18.0 ± .7.8	13.0 ± 20.8	173 ± 112	3.6 ± 3.5	5.4 ± 4.1	6.1 ± 2.5	7.4 ± 2.3	266 ± 290	0 ± 12.7	0 ± 798	6.6 ± 19.0
DES ($n = 71$)	23.0 ± 6.0**	13.0 ± 24.5	222 ± 121**	3.7 ± 2.6	5.7 ± 2.4	4.9 ± 2.8**	6.2 ± 2.8*	156 ± 166*	4.6 ± 11.6	315 ± 665	33.0 ± 40.5*
LST + VLST											
BMS ($n = 39$)	16.0 ± 7.5	12.0 ± 16.5	173 ± 105	3.3 ± 3.8	5.7 ± 4.3	6.2 ± 2.6	7.7 ± 2.4	289 ± 306	0 ± 13.4	0 ± 868	2.2 ± 15.2
DES ($n = 58$)	23.0 ± 6.0**	10.5 ± 23	225 ± 110**	3.3 ± 2.5	5.6 ± 2.5	5.1 ± 3.0*	6.3 ± 3.1*	187 ± 137*	4.3 ± 10.6	330 ± 650	28.0 ± 40.8*

A + SAST, acute + sub-acute stent thrombosis; BMS, bare metal stent; DES, drug-eluting stent; ER, edge related; IS, intra-stent; L + VLST, late + very late stent thrombosis; Lum., Lumen; Min., minimal; NA, neoatherosclerosis; NI, neointima; NIH, neointimal hyperplasia.
*$P < 0.001$ by U Mann–Whitney test.
**$P < 0.05$ by U Mann–Whitney test.

The main findings were: (i) use of OCT identified an underlying morphological abnormality associated with ST in 97% of the cases; (ii) malapposition and neoatherosclerosis rupture were the main causes of LST and VLST and (iii) Malapposition and underexpansion were prominent mechanisms for AST and SAST.

There was no difference between BMS and DES in the distribution of ST types. Optical coherence tomography was of diagnostic quality in 97% of the cases. This high rate is potentially explained by the frequent use of a two-step approach, i.e. initial treatment of the culprit lesion followed by deferred intra-coronary imaging after optimal medical therapy.[13] This strategy reduces the thrombus load that could interfere with struts analysis[21] and allows improved device and lesion visualization, enhancing the diagnostic value of OCT. It may also explain the discrepancies between the frequencies of ST mechanisms we observed and those in previous reports.[4,9,22] Although we identified a high incidence of severe stent underexpansion among patients with early ST (AST + SAST), malapposition was the main mechanism in this group, as described in the MOST study.[9] These data might reflect the different mechanisms causing malapposition, depending on the timing of diagnosis by OCT. Malapposition can happen during index PCI as a result of inadequate stent expansion (acute malapposition), or appear subsequently due to vessel remodelling (late-acquired malapposition) with DES. In some cases, malapposition may appear after implantation of a stent in an unstable lesion. The mechanisms for the malapposition may be due to the presence of thrombus confined between struts and vessel wall that dissolves over time, difficulties to achieve correct culprit lesion sizing or necrotic deterged plaque coverage.[23] Recent observations indicate that most of the acute strut malapposition resolve spontaneously over time, yet up to 30% do not (late-persistent malapposition).[24] Interestingly, we observed that the incidence of malapposition was elevated in both A + SAST and L + VLST groups and the percentage of malapposed struts, as well as the average maximal distance between struts and vessel wall, were high. Although the underlying causes of ST in our patients were broadly heterogeneous, the results implicate strut malapposition as a causal substrate for ST onset, irrespective of its origin (acute, late-persistent, or late-acquired). We were not able to distinguish late-persistent from late-acquired malapposition among the L + VLST patients in a single time point OCT analysis, which limits our interpretation of the data. Because of enhanced visualization of deeper tissues, intra-vascular ultrasound (IVUS) may be better for the evaluation of positive remodelling[25] which is implicated in late-acquired malapposition. Since IVUS was not used in our study, information on vessel remodelling is not available. However, the high percentage of struts malapposition and stent underexpansion we observed in A + SAST patients is a sign of a need for early detection and correction of these pitfalls during initial PCI, potentially by using intra-vascular imaging. Whether OCT-guided PCI could improve outcomes in this situation is currently under investigation in a randomised prospective clinical trial.[19]

In contrast to other reports,[6,22] we found that ruptured neoatherosclerosis, although common, was not the most frequent cause of VLST. Ruptured neoatherosclerosis was more frequent in BMS than in DES stents. It accounted for 36% of the BMS ST, which is in line with previous reports.[26,27] Neoatherosclerosis formation is related to endothelial dysfunction and chronic inflammation around stent struts, potentially enhanced by the presence of coating polymers.[28] Hence, DES may be more prone to neoatherosclerosis than BMS and may enhance lesion formation.[28] That we nevertheless observed a higher incidence of ruptured neoatherosclerotic lesions in the BMS group is probably explained by the longer duration between index PCI to ST in these patients compared with the DES group.

Stent thrombosis remains a therapeutic challenge for the clinician and there are no current international guidelines to guide treatment.[20] The lack of consensus reflects a weak evidence base reflecting the lack of randomized controlled trials for what is a rare spontaneous event. The diagnostic challenges, including use (or not) of intra-vascular imaging and the heterogeneity of aetiologies, collectively contribute to our incomplete understanding of the causes and treatment of ST. Establishing an accurate diagnosis for the cause of ST is necessary in order to implement appropriate therapy. In our series, physicians reported that the ST origin could be identified with certainty by angiography in only 12% of cases whereas this percentage rose to 41% with OCT analysis, pointing out the very poor specificity of angiographic tools to assess ST aetiology. Balloon angioplasty and medical treatment alone were provided in 37 and 29% of the cases, respectively. Redo stent implantation was used in 31.1% of the cases, which is lower than in other published works. In a series of 7135 ST analysed by angiography, Armstrong and colleagues reported use of redo stenting in >50% of cases.[29] The lower rate of stenting in patients managed with adjunctive OCT reflects on the added diagnostic value of this technique. For example, alternatives to routine stent implantation include balloon angioplasty alone for severe underexpansion or subsequent stent placement for neoatherosclerosis or edge-related disease progression.

We observed a relatively low rate of adverse events in the PESTO population, which might be explained by a number of factors. First, our cohort includes a high percentage of patients with VLST, a condition that is associated with a better prognosis than early ST.[29] Moreover, some patients presenting with pre-procedural cardiac arrest or cardiogenic shock were not screened or included in our final analysis, which probably decreased the number of adverse events. Furthermore, the high adoption of thrombus aspiration devices and GPIIb–IIIa inhibitors may also be relevant. Whether the reduced need for redo stenting from the OCT analysis contributed to these results cannot be determined in the present analysis and remains to be proven.

Several limitations of this study deserve consideration. First, ST is a multifactorial process that potentially involves stent architecture abnormality and clinical factors, including degree of platelet inhibition under therapy or compliance with treatment. Although we evaluated declared compliance with APT, we do not have data regarding platelet function or genetic testing in our population, since the different tests were not performed routinely in the different centres. Moreover, a substantial number of patients presenting with ST were not screened for inclusion in the study because of an inadequate clinical presentation or impossibility to restore TIMI 3 flow without PCI before OCT images acquisition. Thus, our results might be biased by patient selection and not reflect the true incidence of the different ST mechanisms in the general population (229 ST during this period in the 17 active centres). Moreover, our approach to OCT analysis was based on a core laboratory analysis

and consensus between three expert operators. This approach might create some discrepancies in case of multiple underlying abnormalities (such as underexpansion and malapposed struts or evaginations and uncovered struts), yet there are currently no guidelines available to help resolve this issue. Furthermore, most of the OCT data in the present study were acquired during a deferred procedure following the initial deocclusion, according to the operators' discretion. This fact might explain the low rate of OCT acquisitions that were rejected for inadequate quality by the corelab. However, our data might differ from series in which the intra-coronary imaging analysis was not deferred and thus make generalization of our conclusions more difficult.

Other limitations are the absence of an IVUS assessment at the time of the ST, the lack of thrombus aspirate analysis and the heterogeneity of the types of stent used. Finally, the PESTO registry was designed to analyse the incidences of characteristics of ST in the French population. There was no control group of patients with non-thrombotic stent analysed with OCT that would have allowed us to specifically investigate predictive factors for ST, including the role of uncovered struts.

In conclusion, in this prospective registry in France, most ST events occurred $\geq$1 year after the initial procedure. Optical coherence tomography identified an underlying morphological abnormality in 97% of cases. Although the underlying mechanisms were various, struts malapposition, ruptured neoatherosclerosis, and severe underexpansion were the most frequently observed causes.

Authors' contributions

A.N., M.A. performed statistical analysis. A.N., S.G. handled funding and supervision. S.G., A.N., M.P., C.X., M.N., M.L., V.G., C.G., B.P., T.C., R.G., R.G., L.S., T.E., D.R., D.O., L.T., B.L. acquired the data. S.G., A.N., M.P. conceived and designed the research. S.G., A.N. drafted the manuscript. S.G., A.N. made critical revision of the manuscript for key intellectual content.

Funding

This work received unrestricted financial support from Saint-Jude Medical and Medtronic.

Conflict of interest: G.S., P.M.: consulting for St Jude Medical and Terumo; N.A., C.C. consulting for St Jude Medical.

References

1. Räber L, Magro M, Stefanini GG, Kalesan B, van Domburg RT, Onuma Y, Wenaweser P, Daemen J, Meier B, Jüni P, Serruys PW, Windecker S. Very late coronary stent thrombosis of a newer-generation everolimus-eluting stent compared with early-generation drug-eluting stents: a prospective cohort study. *Circulation* 2012;**125**:1110–1121.
2. van Werkum JW, Heestermans AA, Zomer AC, Kelder JC, Suttorp M-J, Rensing BJ, Koolen JJ, Brueren BRG, Dambrink J-HE, Hautvast RW, Verheugt FW, ten Berg JM. Predictors of coronary stent thrombosis: the Dutch stent thrombosis registry. *J Am Coll Cardiol* 2009;**53**:1399–1409.
3. Kimura T, Morimoto T, Kozuma K, Honda Y, Kume T, Aizawa T, Mitsudo K, Miyazaki S, Yamaguchi T, Hiyoshi E, Nishimura E, Isshiki T, RESTART Investigators. Comparisons of baseline demographics, clinical presentation, and long-term outcome among patients with early, late, and very late stent thrombosis of sirolimus-eluting stents: observations from the registry of stent thrombosis for review and reevaluation (RESTART). *Circulation* 2010;**122**:52–61.
4. Prati F, Kodama T, Romagnoli E, Gatto L, Di Vito L, Ramazzotti V, Chisari A, Marco V, Cremonesi A, Parodi G, Albertucci M, Alfonso F. Suboptimal stent deployment is associated with subacute stent thrombosis: optical coherence tomography insights from a multicenter matched study. From the CLI Foundation investigators: the CLI-THRO study. *Am Heart J* 2015;**169**:249–256.
5. Nakazawa G, Vorpahl M, Finn AV, Narula J, Virmani R. One step forward and two steps back with drug-eluting-stents: from preventing restenosis to causing late thrombosis and nouveau atherosclerosis. *JACC Cardiovasc Imaging* 2009;**2**:625–628.
6. Amabile N, Souteyrand G, Ghostine S, Combaret N, Slama MS, Barber-Chamoux N, Motreff P, Caussin C. Very late stent thrombosis related to incomplete neointimal coverage or neoatherosclerotic plaque rupture identified by optical coherence tomography imaging. *Eur Heart J Cardiovasc Imaging* 2014;**15**:24–31.
7. Guagliumi G, Sirbu V, Musumeci G, Gerber R, Biondi-Zoccai G, Ikejima H, Ladich E, Lortkipanidze N, Matiashvili A, Valsecchi O, Virmani R, Stone GW. Examination of the in vivo mechanisms of late drug-eluting stent thrombosis: findings from optical coherence tomography and intravascular ultrasound imaging. *JACC Cardiovasc Interv* 2012;**5**:12–20.
8. Hassan AK, Bergheanu SC, Stijnen T, van der Hoeven BL, Snoep JD, Plevier JW, Schalij MJ, Wouter Jukema J. Late stent malapposition risk is higher after drug-eluting stent compared with bare-metal stent implantation and associates with late stent thrombosis. *Eur Heart J* 2010;**31**:1172–1180.
9. Parodi G, La Manna A, Di Vito L, Valgimigli M, Fineschi M, Bellandi B, Niccoli G, Giusti B, Valenti R, Cremonesi A, Biondi-Zoccai G, Prati F. Stent-related defects in patients presenting with stent thrombosis: differences at optical coherence tomography between subacute and late/very late thrombosis in the mechanism of stent thrombosis (MOST) study. *EuroIntervention* 2013;**9**:936–944.
10. Authors/Task Force Members, Windecker S, Kolh P, Alfonso F, Collet JP, Cremer J, Falk V, Filippatos G, Hamm C, Head SJ, Juni P, Kappetein AP, Kastrati A, Knuuti J, Landmesser U, Laufer G, Neumann FJ, Richter DJ, Schauerte P, Sousa Uva M, Stefanini GG, Taggart DP, Torracca L, Valgimigli M, Wijns W, Witkowski A. 2014 ESC/EACTS Guidelines on myocardial revascularization: The Task Force on Myocardial Revascularization of the European Society of Cardiology (ESC) and the European Association for Cardio-Thoracic Surgery (EACTS) Developed with the special contribution of the European Association of Percutaneous Cardiovascular Interventions (EAPCI). *Eur Heart J* 2014;**35**:2541–2619.
11. Cutlip DE, Windecker S, Mehran R, Boam A, Cohen DJ, van Es G-A, Gabriel Steg P, Morel M-al, Mauri L, Vranckx P, McFadden E, Lansky A, Hamon M, Krucoff MW, Serruys PW, Academic Research Consortium. Clinical end points in coronary stent trials. *Circulation* 2007;**115**:2344–2351.
12. Task Force on the Management of STseamiotESoC, Steg PG, James SK, Atar D, Badano LP, Blomstrom-Lundqvist C, Borger MA, Di Mario C, Dickstein K, Ducrocq G, Fernandez-Aviles F, Gershlick AH, Giannuzzi P, Halvorsen S, Huber K, Juni P, Kastrati A, Knuuti J, Lenzen MJ, Mahaffey KW, Valgimigli M, van't Hof A, Widimsky P, Zahger D. ESC Guidelines for the management of acute myocardial infarction in patients presenting with ST-segment elevation. *Eur Heart J* 2012;**33**:2569–2619.
13. Souteyrand G, Amabile N, Combaret N, Hammas S, Prati F, Berry C, Pereira B, Lusson JR, Caussin C, Motreff P. Invasive management without stents in selected acute coronary syndrome patients with a large thrombus burden: a prospective study of optical coherence tomography guided treatment decisions. *EuroIntervention* 2015;**11**:319–324.
14. Prati F, Regar E, Mintz GS, Arbustini E, Di Mario C, Jang IK, Akasaka T, Costa M, Guagliumi G, Grube E, Ozaki Y, Pinto F, Serruys PW. Expert review document on methodology, terminology, and clinical applications of optical coherence tomography: physical principles, methodology of image acquisition, and clinical application for assessment of coronary arteries and atherosclerosis. *Eur Heart J* 2010;**31**:401–415.
15. Prati F, Guagliumi G, Mintz GS, Costa M, Regar E, Akasaka T, Barlis P, Tearney GJ, Jang I-K, Arbustini E, Bezerra HG, Ozaki Y, Bruining N, Dudek D, Radu M, Erglis A, Motreff P, Alfonso F, Toutouzas K, Gonzalo N, Tamburino C, Adriaenssens T, Pinto F, Serruys PWJ, Di Mario C, Expert's OCT Review Document. Expert review document part 2: methodology, terminology and clinical applications of optical coherence tomography for the assessment of interventional procedures. *Eur Heart J* 2012;**33**:2513–2520.
16. Prati F, Capodanno D, Pawlowski T, Ramazzotti V, Albertucci M, La Manna A, Di Salvo M, Gil RJ, Tamburino C. Local delivery versus intracoronary infusion of abciximab in patients with acute coronary syndromes. *JACC Cardiovasc Interv* 2010;**3**:928–934.
17. Radu MD, Raber L, Kalesan B, Muramatsu T, Kelbaek H, Heo J, Jorgensen E, Helqvist S, Farooq V, Brugaletta S, Garcia-Garcia HM, Juni P, Saunamaki K, Windecker S, Serruys PW. Coronary evaginations are associated with positive vessel remodelling and are nearly absent following implantation of newer-generation drug-eluting stents: an optical coherence tomography and intravascular ultrasound study. *Eur Heart J* 2014;**35**:795–807.
18. Kang SJ, Mintz GS, Akasaka T, Park DW, Lee JY, Kim WJ, Lee SW, Kim YH, Whan Lee C, Park SW, Park SJ. Optical coherence tomographic analysis of in-stent neoatherosclerosis after drug-eluting stent implantation. *Circulation* 2011;**123**:2954–2963.

19. Meneveau N, Ecarnot F, Souteyrand G, Motreff P, Caussin C, Van Belle E, Ohlmann P, Morel O, Grentzinger A, Angioi M, Chopard R, Schiele F. Does optical coherence tomography optimize results of stenting? Rationale and study design. *Am Heart J* 2014;**168**:175–81 e1–2.
20. Alfonso F, Sandoval J. New insights on stent thrombosis: in praise of large nation-wide registries for rare cardiovascular events. *JACC Cardiovasc Interv* 2012;**5**: 141–144.
21. Amabile N, Hammas S, Fradi S, Souteyrand G, Veugeois A, Belle L, Motreff P, Caussin C. Intra-coronary thrombus evolution during acute coronary syndrome: regression assessment by serial optical coherence tomography analyses. *Eur Heart J Cardiovasc Imaging* 2015;**16**:433–440.
22. Kang S-J, Lee CW, Song H, Ahn J-M, Kim W-J, Lee J-Y, Park D-W, Lee S-W, Kim Y-H, Mintz GS, Park S-W, Park S-J. OCT analysis in patients with very late stent thrombosis. *JACC Cardiovasc Imaging* 2013;**6**:695–703.
23. Gonzalo N, Barlis P, Serruys PW, Garcia-Garcia HM, Onuma Y, Ligthart J, Regar E. Incomplete stent apposition and delayed tissue coverage are more frequent in drug-eluting stents implanted during primary percutaneous coronary intervention for ST-segment elevation myocardial infarction than in drug-eluting stents implanted for stable/unstable angina: insights from optical coherence tomography. *JACC Cardiovasc Interv* 2009;**2**:445–452.
24. Shimamura K, Kubo T, Akasaka T, Kozuma K, Kimura K, Kawamura M, Sumiyoshi T, Ino Y, Yoshiyama M, Sonoda S, Igarashi K, Miyazawa A, Uzui H, Sakanoue Y, Shinke T, Morino Y, Tanabe K, Kadota K, Kimura T. Outcomes of everolimus-eluting stent incomplete stent apposition: a serial optical coherence tomography analysis. *Eur Heart J Cardiovasc Imaging* 2015;**16**:23–28.
25. Inaba S, Mintz GS, Farhat NZ, Fajadet J, Dudek D, Marzocchi A, Templin B, Weisz G, Xu K, de Bruyne B, Serruys PW, Stone GW, Maehara A. Impact of positive and negative lesion site remodeling on clinical outcomes: insights from PROSPECT. *JACC Cardiovasc Imaging* 2014;**7**:70–78.
26. Hou J, Qi H, Zhang M, Ma L, Liu H, Han Z, Meng L, Yang S, Zhang S, Yu B, Jang I-K. Development of lipid-rich plaque inside bare metal stent: possible mechanism of late stent thrombosis? An optical coherence tomography study. *Heart* 2010;**96**: 1187–1190.
27. Yamaji K, Inoue K, Nakahashi T, Noguchi M, Domei T, Hyodo M, Soga Y, Shirai S, Ando K, Kondo K, Sakai K, Iwabuchi M, Yokoi H, Nosaka H, Nobuyoshi M, Kimura T. Bare metal stent thrombosis and in-stent neoatherosclerosis. *Circ Cardiovasc Interv* 2012;**5**:47–54.
28. Otsuka F, Byrne RA, Yahagi K, Mori H, Ladich E, Fowler DR, Kutys R, Xhepa E, Kastrati A, Virmani R, Joner M. Neoatherosclerosis: overview of histopathologic findings and implications for intravascular imaging assessment. *Eur Heart J* 2015; **36**:2147–2159.
29. Armstrong EJ, Feldman DN, Wang TY, Kaltenbach LA, Yeo K-K, Wong SC, Spertus J, Shaw RE, Minutello RM, Moussa I, Ho KKL, Rogers JH, Shunk KA. Clinical presentation, management, and outcomes of angiographically documented early, late, and very late stent thrombosis. *JACC Cardiovasc Interv* 2012;**5**:131–140.